Kaposi's Sarcoma-Associated Herpesvirus MicroRNA Single-Nucleotide Polymorphisms Identified in Clinical Samples Can Affect MicroRNA Processing, Level of Expression, and Silencing Activity

Soo-Jin Han,[a] Vickie Marshall,[b] Eugene Barsov,[b] Octavio Quiñones,[c] Alex Ray,[b] Nazzarena Labo,[b] Matthew Trivett,[b] David Ott,[b] Rolf Renne,[a] Denise Whitby[b]

Department of Molecular Genetics and Microbiology, University of Florida, Gainesville, Florida, USA[a]; AIDS and Cancer Virus Program, SAIC—Frederick, Frederick National Laboratory for Cancer Research, Frederick, Maryland, USA[b]; Computer and Statistical Services, Frederick National Laboratory for Cancer Research, Frederick, Maryland, USA[c]

Kaposi's sarcoma-associated herpesvirus (KSHV) encodes 12 pre-microRNAs that can produce 25 KSHV mature microRNAs. We previously reported single-nucleotide polymorphisms (SNPs) in KSHV-encoded pre-microRNA and mature microRNA sequences from clinical samples (V. Marshall et al., J. Infect. Dis., 195:645–659, 2007). To determine whether microRNA SNPs affect pre-microRNA processing and, ultimately, mature microRNA expression levels, we performed a detailed comparative analysis of (i) mature microRNA expression levels, (ii) in vitro Drosha/Dicer processing, and (iii) RNA-induced silencing complex-dependent targeting of wild-type (wt) and variant microRNA genes. Expression of pairs of wt and variant pre-microRNAs from retroviral vectors and measurement of KSHV mature microRNA expression by real-time reverse transcription-PCR (RT-PCR) revealed differential expression levels that correlated with the presence of specific sequence polymorphisms. Measurement of KSHV mature microRNA expression in a panel of primary effusion lymphoma cell lines by real-time RT-PCR recapitulated some observed expression differences but suggested a more complex relationship between sequence differences and expression of mature microRNA. Furthermore, in vitro maturation assays demonstrated significant SNP-associated changes in Drosha/DGCR8 and/or Dicer processing. These data demonstrate that SNPs within KSHV-encoded pre-microRNAs are associated with differential microRNA expression levels. Given the multiple reports on the involvement of microRNAs in cancer, the biological significance of these phenotypic and genotypic variants merits further studies in patients with KSHV-associated malignancies.

Kaposi's sarcoma (KS)-associated herpesvirus (KSHV) causes KS (1) and primary effusion lymphoma (PEL) (2) and is associated with a subset of multicentric Castleman's disease (MCD) (3).

MicroRNAs are small single-stranded RNAs averaging 22 nucleotides (nt) in length which posttranscriptionally regulate gene expression primarily by targeting 3′ untranslated regions of mRNAs. MicroRNA targeting of mRNAs inhibits translation, subsequently leading to mRNA decay. MicroRNAs are processed from precursor polymerase II (Pol II) transcripts by two types of RNA III endonucleases. In the nucleus, precursors of mature microRNAs before Drosha cleavage (pri-microRNAs) form a hairpin, which is cleaved at the base by Drosha/DGCR8. The resulting pre-microRNA (after Drosha cleavage) is efficiently exported into the cytoplasm, where it is recognized by Dicer, which cleaves the hairpin bulge to generate a double-stranded RNA molecule. Usually, one strand, the mature microRNA, is then incorporated into the RNA-induced silencing complex (RISC). For some human and many viral microRNAs, both strands can be incorporated into RISC with various efficiencies (for a review, see references 4 and 5).

Virally encoded microRNAs were first discovered in Epstein-Barr virus (EBV)-infected Burkitt's lymphoma cells (6) and have subsequently been identified in many alpha-, beta-, and gammaherpesviruses (reviewed in reference 7). KSHV encodes 12 pre-microRNAs that give rise to 25 mature microRNAs (6, 8–12). KSHV-encoded microRNAs are located within the latency-associated region and are expressed at different levels in all KSHV-associated malignancies (13, 14). Ten microRNAs are expressed as a cluster and located between the viral FLIP and kaposin genes, while the remaining two are embedded within the K12 open reading frame.

We recently investigated the sequence conservation of the KSHV-encoded microRNA region in KSHV-infected PEL cell lines and clinical samples from patients with KS and MCD. We observed that while the region was generally highly conserved, a distinct cluster of sequences showed substantial divergence (15). We also observed single-nucleotide polymorphisms (SNPs) or multiple-nucleotide polymorphisms in pre-microRNA sequences of K12-2, -4, -5, -6, -7, -9, and -10. In subsequent studies, detailed analysis of SNPs in the KSHV microRNA-coding region suggested an association with a risk of AIDS-associated KS (16), MCD, and KSHV-associated inflammatory cytokine syndrome (KICS) (17), a more recently described condition associated with an extremely high viral load (18). An earlier study, using in vitro maturation assays, reported that an SNP observed in the precursor stem-loop of K12 microRNA 5 (miR-K12-5) affects Drosha processing and subsequent mature microRNA expression in PEL cell lines (19).

In the current study, we systematically analyzed the effect of SNPs in multiple KSHV pre-microRNAs on microRNA process-

ing, expression, and targeting using complementary molecular approaches. First, HEK293T cells were transduced with retroviral vectors expressing either KSHV wild type (wt) or variant (v) pre-microRNAs derived from sequences observed in clinical samples and mature microRNA expression was determined using reverse transcription (RT)-quantitative PCR (qPCR) with an ABI system. Second, we characterized the expression of variant microRNAs present in PEL cell lines using RT-qPCR with an ABI system. Third, *in vitro* maturation assays were performed to assess SNP-dependent differences in Drosha/DGCR8 and Dicer processing. Lastly, we performed reporter assays using microRNA sensor vectors, which demonstrated that SNP-dependent expression/maturation differences indeed translate into variable silencing efficiency. Together, these data indicate that the KSHV-encoded SNPs observed in pre-microRNAs may have phenotypic consequences for viral biology and pathogenesis.

MATERIALS AND METHODS

Cell lines. HEK293T human embryonic kidney cells were obtained from the American Type Culture Collection and maintained in Dulbecco's modified Eagle's medium (DMEM; Mediatech) supplemented with 10% fetal bovine serum (FBS; Mediatech), 2 mM L-glutamine, and penicillin-streptomycin (5 U/ml and 5 μg/ml, respectively; Mediatech). Cells of a panel of KSHV-positive primary effusion lymphoma cell lines (BCBL-1, JSC-1, BCP-1, VG-1, BC-1, BC-2, BC-3) were grown in RPMI 1640 (Life Technologies) containing 10% FBS (Atlantic Biologicals) and 1% penicillin-streptomycin-glutamine (Life Technologies).

KSHV copy number quantification by real-time PCR. KSHV copy numbers in PEL cell lines were determined using approximately 250 ng total DNA per reaction mixture in triplicate, as previously reported (20). Cell quantification was determined using a quantitative real-time PCR assay for human endogenous retrovirus 3 (ERV-3) (21) to allow the number of KSHV copies per cell to be calculated.

PEL cell line sequencing and analysis. The sequence of the KSHV-encoding microRNA region as well as a fragment of K12 containing the sequences for miR-K12-10 and -12 were previously reported for the PEL cell lines BC-1, BC-2, BCBL-1, BCP-1, and JSC-1 (15). The same regions were amplified and sequenced from two additional cell lines, BC-3 and VG-1, as previously described (15).

Retroviral vectors expressing KSHV wt and variant microRNAs. BCBL-1 was designated the wild type because it is commonly used as a model for KSHV research and it has a KSHV microRNA sequence that was found to cluster in the conserved arm of the phylogenetic tree in our previous study (15). KSHV wt and variant pre-microRNA sequences were amplified from previously characterized clinical samples using *Pfu* DNA polymerase (Stratagene), with the exception of wt pre-microRNA K12-6, which was synthesized (Operon) (16). The pre-microRNAs included in this study are listed in Table 1. The pre-microRNA sequences were amplified using primers with adapters that introduced 5′ BamHI and 3′ EcoRI restriction sites for directional cloning into the RNA interference-ready pSIREN-retroQ-DsRed-Express vector (Clontech). All constructs were verified by sequencing. The primers used for amplification of pre-microRNA sequences are listed in Table 2, and the forward primer sequences used for custom small RNA real-time PCR assays are given in Table 3. The vector construct, including the amplified and cloned wt and V pre-microRNA sequences, is shown in Fig. 1.

The retroviral vector stocks were made using GP2-293 packaging cells (Clontech) cotransfected with the pSIREN-KSHV plasmid DNA and a vesicular stomatitis virus envelope G glycoprotein (VSV-G)-expressing construct plasmid using the Transit-293 transfection reagent, as recommended by the manufacturer (Mirus Bio). Supernatants were harvested at 48 h posttransfection, and retroviral particles were concentrated by centrifugation, as previously described (22). Transduced HEK293T cells were

expanded for 2 weeks in selection medium, after which the cells were sorted for DsRed expression.

To measure the transduction efficiency in HEK293T cells, quantitative RT-PCR for the DsRed gene was performed. Primers and probes were designed using Primer Express (version 3.0) software (Applied Biosystems) according to recommended guidelines and are as follows: primer DsRedqPCR-F, 5′-GCAGGACGGCTCCTTCATC-3′; primer DsRedqPCR-R, 5′-CAGCCCATAGTCTTCTTCTGCAT-3′; and DsRedqPCR-probe, 5′-FAM-AGGTGAAGTTCATCGGC-TAMRA-3′, where FAM is 6-carboxyfluorescein and TAMRA is 6-carboxytetramethylrhodamine.

For quantification, a standard curve was generated using serially diluted circularized pSIREN vector DNA. All assays were performed using an ABI Prism 7900HT sequence detection system. RNA from transduced 293T cells was reverse transcribed to cDNA using a high-capacity cDNA reverse transcription kit (Applied Biosystems) and a DsRed-specific RT primer, DsRedCP-R (5′-TTCAGCTTCAGGGCCTTGTG-3′). The resulting cDNA was then screened using the aforementioned DsRed qPCR assay. Replicates of each HEK293T-KSHV microRNA transduction were tested in triplicate, and the threshold cycle (C_T) values of the independent replicates were averaged.

RNA extraction from cell lines latently infected with KSHV and HEK293T transductions. The isolation of RNA from HEK293T transductions and PEL cells was performed using the TRIzol reagent (Invitrogen) per the manufacturer's instructions, and the RNA was quantified using a Nanodrop 1000 spectrophotometer (Thermo Scientific).

Analysis of KSHV microRNA expression in PEL and retrovirus-transduced HEK293T cells. Mature KSHV microRNA expression was determined using TaqMan small RNA assays (Applied Biosystems). The sequence of the mature microRNA was used to design each custom assay, which included a specific stem-looped RT primer, and TaqMan qPCR assay. A total of 21 custom assays were designed on the basis of the wt and variant microRNA sequences (Table 2). Human small nuclear RNAs RNU6B and RNU48 were used as endogenous controls to normalize for RNA input. All samples were tested multiple times in triplicate reactions, and the C_T values of the replicates were averaged. For experiments with HEK293T cells, untransduced HEK293T cells were used as a negative control in quantitative RT-PCR assays and consistently gave C_T values of 40. All qPCRs were performed using an ABI Prism 7900HT sequence detector system.

Statistical analyses. Statistical analyses for the gene expression data obtained from real-time qPCR analysis were performed using Spotfire S+, version 8.0, software (TIBCO Spotfire, Somerville, MA). The target genes (microRNAs) were first normalized to the host microRNA, RNU6B, and then the fold changes were computed via the $2^{-\Delta\Delta CT}$ method (23). For PEL cell lines BCP-1, VG-1, JSC-1, BC-1, BC-2, and BC-3, changes relative to the value for the wild-type BCBL-1 cell line were computed. Box-and-whisker plots depict raw C_T gene expression values for HEK293T cells for each microRNA variant and the wt and indicate evidence of either differences between the microRNA variants and the wt or a lack thereof. Nonparametric/distribution-free Wilcoxon rank-sum tests were performed to confirm possible differences between SNP and wt microRNAs, as observed in Fig. 1. P values of less than 0.01 were considered significant (Fig. 1).

***In vitro* microRNA maturation assay.** MicroRNA *in vitro* maturation assays were performed as described by Lee and Kim (24). All wt and variant pre-microRNAs tested were transcribed from T7 promoter-containing pcDNA3.1/V5/HisA vectors, as previously described (25). For microRNA maturation assays, plasmids were linearized prior to *in vitro* transcription using T7 polymerase in the presence of [α-^{32}P]UTP. Radiolabeled transcripts were separated on a 6% urea-polyacrylamide gel and extracted from the gel in elution buffer (0.3 M sodium acetate [pH 5.5], 2% SDS) at 42°C overnight. Recovered size-selected RNA was precipitated and resuspended in RNase-free TE (Tris-EDTA) buffer. Recombinant plasmids expressing pCK-Drosha (Flag) and pCK-DGCR8 (Flag) were kind gifts from Narry Kim, Seoul National University, Seoul, Republic of

TABLE 1 wt and variant microRNAs previously observed in clinical samples from patients with KSHV-associated cancers and present in PEL cell lines included in this study

KSHV miRNA	Location of SNP	Pre-microRNA M-fold diagram[a]	KSHV cell line(s) latently infected with microRNA
miR-K12-5v[b]	Pre-microRNA	(M-fold diagram)	BC-1, VG-1
miR-K12-5wt		(M-fold diagram)	BCBL-1, BC-2, BC-3, BCP-1, JSC-1
miR-K12-9sv[c]	Pre-microRNA	(M-fold diagram)	VG-1
miR-K12-4v[c]	Terminal loop	(M-fold diagram)	VG-1
miR-K12-4wt		(M-fold diagram)	BCBL-1, BC-1, BC-2, BC-3, BCP-1, JSC-1
miR-K12-7v[c]	Terminal loop	(M-fold diagram)	VG-1
miR-K12-7wt		(M-fold diagram)	BCBL-1, BC-1, BC-2, BC-3, BCP-1, JSC-1
miR-K12-10v[c]	Terminal loop	(M-fold diagram)	BC-1
miR-K12-10wt		(M-fold diagram)	BCBL-1, BC-2, BC-3, BCP-1, JSC-1, VG-1
miR-K12-2v[d]	Mature microRNA	(M-fold diagram)	
miR-K12-2wt		(M-fold diagram)	BCBL-1, BC-1, BC-2, BC-3, BCP-1, JSC-1
miR-K12-6v[c]	Mature microRNA	(M-fold diagram)	

Pre-microRNA M-fold diagrams:

```
miR-K12-5v
U   UA   -  C  U* GC       G  U AC
 GACC GGUA GU   GGU  CCUAAG G CU  A
 |||| |||| ||   |||  ||||||
 CUGG CCGU CA GG CCG  GGAUUC C GA  U
A   --   U  A  U  UA       A - AC

miR-K12-5wt
U   UA   -  C UA  GC       G  U AC
 GACC GGUA GU CC  GU  CCUAAG G CU  A
 |||| |||| ||     |||  ||||||
 CUGG CCGU CA GG  CG  GGAUUC C GA  U
A   --   U  A UC  UA       A - AC

miR-K12-9sv
 *
 A        C            A    C    C U
GGGU UAC CAGCUGCGUA ACCC GCUG G  A
|||| ||| |||||||||| |||| |||| |
CCCA AUG GUCGACGCAU UGGG CGAC C  A
     A   C            A    U     A A

miR-K12-4v
   C        AA  G     C    --G   UU *
AUAA UAGCUA   CC CAGUA UCUA   GGCA  U
|||| ||||||   || ||||| ||||   ||||
UAUU GUCGAU   GG GUCAU AGAU   UUGU  A
                              ACA  UU
   A        CC  A     A

miR-K12-4wt
   C        AA  G     C    --G   UU
AUAA UAGCUA   CC CAGUA UCUA   GGCA  C
|||| ||||||   || ||||| ||||   ||||
UAUU GUCGAU   GG GUCAU AGAU   UUGU  A
                              ACA  UU
   A        CC  A     A

miR-K12-7v
G  U       C   ACG      U   -CUG
 CGU GAGCGCCA CGG  GGGAUU AUG   UAU
 ||| |||||||| |||  |||||| |||      C
 GCA CUCGCGGU GUU  CCCUAG UAC   AUU
G  -       C   GUA      -   CAUA
                                *

miR-K12-7wt
G  U       C   ACG      U   -CU
 CGU GAGCGCCA CGG  GGGAUU AUG  GUAU
 ||| |||||||| |||  |||||| |||     C
 GCA CUCGCGGU GUU  CCCUAG UAC  CAUU
G  -       C   GUA      -   CAU

miR-K12-10v
   AG      C   C  CAC    UGU *
CUGG GCUUGGGG GAUA CAC UCGUU  G
|||| |||||||| |||| ||| |||||
GACC UGAGCCCC CUGU GUG AGCGG  U
   GG      C   U  AUU    UUG

miR-K12-10wt
   AG      C   C  CAC    UGU
CUGG GCUUGGGG GAUA CAC UCGUU  C
|||| |||||||| |||| ||| |||||
GACC UGAGCCCC CUGU GUG AGCGG  U
   GG      C   U  AUU    UUG

miR-K12-2v
U  C    A  G      G  U*      AGCCAUU    C
 CG UA CU UAGUCC GG  AGAUCUG        GAAG  A
 || || || ||||| ||   ||||||        ||||
 GC GU GA AUCGGG CC UCUAGAC        CUUC  A
C  C   C  G      A  U      -------      G

miR-K12-2wt
U  C    A  G      G  UC      AGCCAUU    C
 CG UA CU UAGUCC GG  GAUCUG        GAAG  A
 || || || ||||| ||   ||||||        ||||
 GC GU GA AUCGGG CC  CUAGAC        CUUC  A
C  C   C  G      A  UU      -------      G

miR-K12-6v
       C      A U -U      GG
CUUGU CAGCAGC CC AA CCAUCGGC  U
||||| ||||||| || || |||||||
GAGCA GUUGUCG GG UU GGUAGUCG  C
     *A      -  C UU      GG
```

(Continued on following page)

TABLE 1 (Continued)

KSHV miRNA	Location of SNP	Pre-microRNA M-fold diagram[a]	KSHV cell line(s) latently infected with microRNA
miR-K12-6wt			BCBL-1, BC-1, BC-2, BC-3, BCP-1, JSC-1, VG-1
miR-K12-9mv[c]	Mature microRNA		BCP-1, BC-3
miR-K12-9wt			BCBL-1, BC-1, JSC-1

```
miR-K12-6wt
          UC          A    U  -U        GG
     CUUG  CAGCAGC CC AA   CCAUCGGC     U
     ||||  ||||||| || ||   ||||||||     
     GAGC  GUUGUCG GG UU   GGUAGUC G     C
          GA         -    C   UU         GG

miR-K12-9mv
          **   *      **  *
        A - TC   TA  -       *      *  *     * UG
     GGGU  A   CAG G GUAUACCCAGGUG GG
     ||||  |    ||| | ||||||||||||| |||
     CCCA  U   GUC  C CAUAUGGGUC GACCC    *  AA
          AA  GC    GA C                 *
                       *

miR-K12-9wt
          C   C          A     C    C  U
     GGGU UAC CAGCUGCGUA ACCC  GCUG  G  A
     |||| ||| |||||||||| ||||  ||||     
     CCCA AUG GUCGACGCAU UGGG  CGAC  C  A
          A   C          A     U    A  A
```

[a] M-Fold diagrams show predominantly expressed microRNAs.
[b] The sequence was first reported by Gottwein et al. (19).
[c] The sequence was first reported by Marshall et al. (15).
[d] The sequence was first reported by Marshall et al. (16).

Korea. Plasmids encoding the Drosha/DGCR8 expression plasmids were cotransfected into HEK293T cells at a ratio of 9:1. Cells were harvested at 48 h posttransfection and lysed in lysis buffer (20 mM Tris-HCl [pH 7.4], 150 mM NaCl, 1 mM EDTA, 0.4% NP-40, proteinase inhibitor cocktail [Sigma]). The Drosha-DGCR8 complex, which is called the microprocessor, was enriched using M2 Flag-tagged agarose beads (Sigma). Radiolabeled wt (BCBL-1) and variant pri-microRNAs were incubated with freshly prepared microprocessor at 37°C for 2 h in reaction buffer (20 mM HEPES [pH 7.6], 10 mM KCl, 0.2 mM EDTA, 5% glycerol). RNA was extracted via phenol-chloroform and ethanol precipitation. After resuspension in RNase-free TE buffer, 50% of the microprocessor-processed RNA was incubated with 1 unit of recombinant turbo Dicer (Genlantis) at 37°C for 2 h.

Products from each step were separated on 10 or 15% urea-polyacrylamide gels and quantified by imaging. Maturation efficiency was determined as a percentage of that for the wild type ± standard deviation from three independent experiments.

Luciferase microRNA reporter assays in HEK293T cells. Luciferase activity was quantified using a dual-luciferase assay system (Promega) according to the manufacturer's protocol. For plasmids expressing individual pri-microRNAs (wt or variants), a region of approximately 200 nt surrounding each pre-microRNA hairpin was amplified from the cluster-containing plasmid and inserted into pcDNA3.1/V5/HisA. Efficient wt microRNA expression from these constructs has previously been demonstrated (25). Individual KSHV microRNA sensor vectors containing two sites with 100% complementary binding to the wt microRNAs down-

TABLE 2 Primers used to amplify KSHV wt and variant pre-microRNA sequences

Pre-microRNA	Orientation	Primer sequence[a] (subtype)
mir-K12-2	Forward	ACACAC-GGATCC-GAAAGTCCGTCAACCAGATT (A/C)
	Forward	ACACAC-GGATCC-GAAAGTCC**A**TCAACCAGATT (B)
	Reverse	ACACAC-GAATTC-TTGGTTGGGAGTTTGGGGAC
mir-K12-4	Forward	ACACAC-GGATCC-CTCCAGGTCCAAGCGACGAAC
	Reverse	ACACAC-GAATTC-GAGGTTTGAGAGGCGTAGACATCC (A/C)
	Reverse	ACACAC-GAATTC-GAGGTTTGAGA**T**GCGTAGACATCC (B)
mir-K12-5	Forward	ACACAC-GGATCC-GGATGTCTACGCCTCTCAAACCTC (A/C)
	Forward	ACACAC-GGATCC-GGATGTCTACGC**A**TCTCAAACCTC (B)
	Reverse	ACACAC-GAATTC-CCCGCATAGGTTTTTGTGGCACC
mir-K12-6	Forward	ACACAC-GGATCC-TAAAGCGGGCGTTCGTAAGCGTG (A/C)
	Forward	ACACAC-GGATCC-TAAAGC**A**GGCGTTCGTAAGCGTG (B)
	Reverse	ACACAC-GAATTC-ACACAGAACAATAACGGGCGACTA
mir-K12-7	Forward	ACACAC-GGATCC-CGTGCCCACCGATGAGATAC
	Reverse	ACACAC-GAATTC-CTACACTAAGCCCGAACG
mir-K12-9	Forward	ACACAC-GGATCC-TGAGTCATCGCAGCCCCTATTC
	Reverse	ACACAC-GAATTC-TGCTTCCGGAAATACCACCTGAGT
mir-K12-10	Forward	ACACAC-GGATCC-GGTGTTTGTGGCAGTTCATGTCC
	Reverse	ACACAC-GAATTC-CGCTAGCTTCAGTGCGCGCCC

[a] Boldface nucleotides indicate SNPs.

TABLE 3 Forward primer sequences used for custom small RNA real-time PCR assays

Mature microRNA	Primer sequences[a]
mir-K12-2	AACUGUAGUCCGGGUCGAUCUG (wt)
	AACUGUAGUCCGGG**U**A**G**AUCUG (v)
mir-K12-4	AGCUAAACCGCAGUACUCUAGG
mir-K12-5	UAGGAUGCCUGGAACUUGCCGG
mir-K12-6	UGAUGGUUUUCGGGCUGUUGAG (wt)
	UGAUGGUUUUCGGGCUGUUGA**A** (v)
mir-K12-7	UGAUCCCAUGUUGCUGGCGC
mir-K12-9	ACCCAGCUGCGUAAACCCCGCU (wt)
	AUCCAG-CU**AGG**UA**U**ACCC**A**GG**U** (v)
mir-K12-10	UAGUGUUGUCCCCCCGAGUGGC

[a] Boldface nucleotides indicate SNPs. Hyphen in sequence for mir-K12-9 represents a deletion.

stream of the luciferase reporter were previously described (11). Expression and sensor vectors were cotransfected with a *Renilla* luciferase vector for normalization. Luciferase activity was analyzed at 72 h posttransfection using a BMG Fluostar luminometer. Each variant microRNA was analyzed using BCBL-1 microRNA as the wt and empty vector as a negative control. Reporter gene activity values represent the means of several independent transfections performed in triplicate, and error bars show the standard deviations from the means.

RESULTS

Comparative expression analysis of HEK 293 cells transduced with retroviral vectors encoding wt or variant microRNAs. Previously, we observed single-nucleotide polymorphisms (SNPs) in pre-microRNA sequences of miR-K12-2, -4, -5, -6, -7, -9, and -10 in clinical samples and PEL cell lines (15, 16). The SNPs evaluated here are summarized in Table 1, which also indicates which SNPs were observed in clinical samples and which were also present in sequences from PEL cell lines. SNPs were observed in various positions within the pre-microRNAs and can be divided into three classes. SNPs in miR-K12-5 and -9sv (where sv represents single variant) were located within the pre-microRNA stem adjacent to the putative Drosha processing site. In miR-K12-4, -7, and -10, SNPs were located within the bulge of the pre-microRNA, which is closer to the Dicer processing site. In miR-K12-2 and -6, the SNPs were located within the mature microRNA, as were some of the multiple SNPs in the highly variant miR-K12-9mv (where mv represents multiple variant), in which multiple SNPs were located throughout the pre-microRNA.

To evaluate the potential impact of these SNPs on processing and expression in a controlled cellular system, we transduced HEK293T cells with retroviral expression vectors encoding either wild-type or variant pre-microRNAs. Cell lines stably expressing these constructs were selected on the basis of DsRed expression. Mature microRNA expression levels were then determined using custom-designed ABI stem-loop real-time PCR assays (Fig. 2).

We showed that SNPs in the pre-microRNA region of miR-K12-5 and -9sv correlate with increased mature microRNA expression (Fig. 2A). In our previous studies of KSHV microRNA-encoded sequences in clinical samples, most subjects were observed to have the miR-K12-5 SNP (15, 16). In contrast, SNPs within the terminal loop region of miR-K12-4 and -7 showed reduced expression. However, not all SNPs in this region resulted in reduced expression, as miR-K12-10 levels were modestly increased (Fig. 2B). MiR-K12-2 had a single SNP in the mature

microRNA, and this correlated with increased expression (Fig. 2C). The SNP in miR-K12-6, however, resulted in reduced mature microRNA expression. The multiple SNPs in miR-K12-9mv, which spanned both arms and the mature microRNA region, resulted in the lowest level of expression of any of the constructs studied (Fig. 2C). Hence, these data demonstrate that SNPs observed within KSHV pre-microRNA genes can affect mature microRNA expression either positively or negatively. The magnitude of these effects varied from very minor to highly significant.

MicroRNA expression analysis in cell lines latently infected with KSHV. In addition to evaluating the effects of SNPs in HEK293T cell lines transduced with individual pre-microRNAs, we also evaluated microRNA expression levels in PEL cells using custom-designed ABI stem-loop real-time PCR assays. In this case, the microRNAs were expressed in the context of the entire pri-microRNA cluster in KSHV-infected cells with all the additional viral genes and viral host cell interaction mechanisms intact. The cell lines tested and the SNPs present are summarized in Table 1.

The levels of expression of seven microRNAs in the different PEL cell lines compared to that in BCBL-1 cells analyzed by the $2^{-\Delta\Delta CT}$ method (23) are shown in Fig. 3. These results show that expression of mature miR-K12-5 is increased in BC-1 cells, as previously reported (19). In addition, increased expression of mature miR-K12-5 was also seen in VG-1 cells, which have the same SNP as that observed in BC-1 cells. However, the increased expression observed in BC-1 cells compared to that observed in BCBL-1 cells was rather modest, and all of the other cell lines, which lacked this SNP, also had increased expression. Similarly, the remaining KSHV pre-microRNAs containing single SNPs (miR-K12-2, -4, -6, -7, and -10) showed varied mature microRNA expression levels between the cell lines in a manner that could not be explained by the presence or absence of the pre-microRNA SNP alone.

In contrast, the multiple SNPs in miR-K12-9 in BC-2, BCP-1, and BC-3 cells spanning both arms of the pre-microRNA correlated with a drastic reduction in mature microRNA expression, which in BCP-1 and BC-3 cells was below the detection level of the assay. The lack of miR-K12-9 expression in BC-3 cells has also been observed by deep sequencing (26). BC-1 and JSC-1 cells both have the wild-type sequence for miR-K12-9. Expression of mature miR-K12-9 was reduced in BC-1 cells but increased in JSC-1 cells compared to the level of expression in BCBL-1 cells. The single SNP in premiR-K12-9-5p (where 5p is the 5′ arm) encoded by VG-1 cells and observed in sequences from many clinical samples (15, 16) also correlates with increased microRNA expression.

These data suggest that the levels of mature microRNA in PEL cells is determined by many factors, in addition to the SNP in the pre-microRNA. This may include differential transcriptional activity between different PEL cells as well as the position of pre-microRNAs within the cluster. Differences in the microRNA processing machinery between HEK293T cells and PEL cells as well as differences between PEL cell lines may also affect processing of viral microRNAs. Sequence analyses of the microRNA-encoding regions from PEL cell lines show many additional SNPs in the pri-microRNA sequence outside the pre-microRNAs, which likely also affect microRNA processing and expression (16, 17).

We observed no correlation between microRNA expression levels and KSHV load. The highest microRNA expression levels were detected in BC-3 cells, which also had the highest viral copy number per cell. However, VG-1 cells also had high microRNA

LTRₓ — P_U6 — pre-miRNA — P_CMV — DsRed — LTRₓ
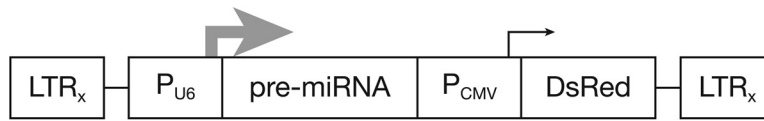
KSHV MiRNA	Amplified and Cloned Pre-microRNA Sequences
miR-K12-2v	GAAAGTCCGTCAACCAGATTTAAGATTAAGATTATAAT**GGGTCTACTTCGCTAACTGTAGTCCG GGTAGATCTGAGCCATTGAAGCAAGCTTCCAGATCTTCCAGGGCTAGAGCTGCCGCGGTGACAC C**AATTATAGAAATTTAGTCCCCAAACTCCCAACCAA
miR-K12-2wt	GAAAGTCCGTCAACCAGATTTAAGATTAAGATTATAAT**GGGTCTACTTCGCTAACTGTAGTCCG GGTCGATCTGAGCCATTGAAGCAAGCTTCCAGATCTTCCAGGGCTAGAGCTGCCGCGGTGACAC C**AATTATAGAAATTTGGTCCCCAAACTCCCAACCAA
miR-K12-4v	CTCCAGGTCCAAGCGACGAACCGCCCGTGGCCACAACGCCGCCTGGTGGAACCGGGCAG T**ATAACTAGCTAAACCGCAGTACTCTAGGGCATTTATTTGTTACATAGAATACTGAGGCCTAGCTGA TTAT**ACTACCTCCGTCCAGCAGTCGACACGGATGTCTACGCTTCTCAAACCTC
miR-K12-4wt	CTCCAGGTCCAAGCGACGAACCGCCCGTGGCCACAACGCCGCCTGGTGGAACCGGGCAG T**ATAACTAGCTAAACCGCAGTACTCTAGGGCATTCATTTGTTACATAGAATACTGAGGCCTAGCTGA TTAT**ACTACCTCCGTCCAGCAGTCGACACGGATGTCTACGCCTCTCAAACCTC
miR-K12-5v	GGATGTCTACGCATCTCAAACCTCGTGGGCACGGCGTCATGACTAAGGGGG**G**AGTT**TGACCTAG GTAGTCCCTGGTGCCCTAAGGGTCTACATCAAGCACTTAGGATGCCTGGAACTTGCCGGTCAAG CCCGCTCA**TAAGACCATAACCTGGTGCCACAAAAACCTATGCGGG
miR-K12-5wt	GGATGTCTACGCCTCTCAAACCTCGTGGGCACGGCGTCATGACTAAGGGGGAGTT**TGACCTAG GTAGTCCCTAGTGCCCTAAGGGTCTACATCAAGCACTTAGGATGCCTGGAACTTGCCGGTCAAG CCCGCTCA**TAAGACCATAACCTGGTGCCACAAAAACCTATGCGGG
miR-K12-6v	TAAAGCAGGCGTTCGTAAGCGTCTGGAACGACACAAACCCTGCGCGGGTCTAGAAAGA**CTTGTC CAGCAGCACCTAATCCATCGGCGGTGCGGGCTGATGGTTTTCGGGCTGTTGAACGAG**TCTT TTTATCTAGTCGCCCGTTATTGTTCTGTGTGT
miR-K12-6wt	TAAAGCGGGCGTTCGTAAGCGTCTGGATCGACACAAACCCTGCGCGGGTTTAGAAAGA**CTTGTC CAGCAGCACCTAATCCATCGGCGGTGCGGGCTGATGGTTTTCGGGCTGTTGAGCGAG**TCTT TTTATCTAGTCGCCCGTTATTGTTCTGTGTGT
miR-K12-7v	CGTGCCCACCGATGAGATACCACGCAGCCGCGCATATTGG**CGTTGAGCGCCACCGGACGG GGATTATGCTGTATCTTAATACCATGATCCCATGTTGCTGGCGCTCACGG**CCCGTGTGCCAGCCG CCTGGACGTCGAAAGCACGCAAAGCTGAACGTTCGGGCTTAGTGTAG
miR-K12-7wt	CGTGCCCACCGATGAGATACCACGCAGCCGCGCATATTGG**CGTTGAGCGCCACCGGACGGG GATTATGCTGTATCTTACTACCATGATCCCATGTTGCTGGCGCTCACGG**CCCGTGTGCCAGCCGCC TGGACGTCGAAAGCACGCAAAGCTGAACGTTCGGGCTTAGTGTAG
miR-K12-9sv	TGAGTCATCGCAGCCCCTATTCCAGTAGGTATACCCAGCT**GGGTATACCCAGCTGCGTAAA CCCCGCTGCGTAAACACAGCTGGGTATACGCAGCTGCGTAAACCC**GGCTGGGTAAATCCAGCTG TAATTCTACAATTAAACAAGGTATAAACCAATGGGGTACTCAGGTGGTATTTCCGGAAGCA
miR-K12-9mv	TGAGTCATCGCAGCCCCTATTCCAGTAGGTATACCCAGCT**GGGTAATCCAGCTAGGTATA CCCAGGTGGGTGAACCCAGCTGGGTATACCCAGCTGCGTAAACCCG**GCTGGGTAAATCCAGCTGT AATTCTACAATTAAACAAGGTATAAACCAATGGGGTACTCAGGTGGTATTTCCGGAAGCA
miR-K12-9wt	TGAGTCATCGCAGCCCCTATTCCAGTAGGTATACCCAGCT**GGGTCTACCCAGCTGCGTAAA CCCCGCTGCGTAAACACAGCTGGGTATACGCAGCTGCGTAAACCC**GGCTGGGTAAATCCAGCTGT AATTCTACAATTAAACAAGGTATAAACCAATGGGGTACTCAGGTGGTATTTCCGGAAGCA
miR-K12-10v	GGTGTTTGTGGCAGTTCATGTCCCGGATGTGTTACTAAATGGGTGGCG**CTGGAGGCTTGGG GCGATACCACCACTCGTTTGTGTGTTGGCGATTAGTGTTGTCCCCCCGAGTGGCCAG**CGTGG CCCCGTAGCATTCAGGACACGAGTTGCAACGGGCGCGCACTGAAGCTAGCG
miR-K12-10wt	GGTGTTTGTGGCAGTTCATGTCCCGGATGTGTTACTAAATGGGTGGCG**CTGGAGGCTTGGG GCGATACCACCACTCGTTTGTCTGTTGGCGATTAGTGTTGTCCCCCCGAGTGGCCAG**CGTGGC CCCGTAGCATTCAGGACACGAGTTGCAACGGGCGCGCACTGAAGCTAGCG

FIG 1 (Top) Diagram of SIREN-RetroQ-DsRed-Express retroviral vector. Large gray arrow, the U6 RNA polymerase III promoter immediately upstream of the cloned pre-microRNA; black arrow, CMV RNA polymerase II promoter expressing DsRed; LTRₓ, self-inactivating long terminal repeats. (Bottom) Cloned sequences of each microRNA (MiRNA), with the mature microRNA being underlined and in bold.

expression, despite having the lowest viral copy number per cell (Fig. 3; Table 4). SNPs in mir-K12-2 and -6, identified in viral sequences from clinical samples (15–17), were not encoded by any of the cell lines tested.

Analysis of Drosha and Dicer processing efficiency of wild-type and variant microRNAs using stepwise *in vitro* maturation assays. The retroviral expression results presented above suggest that the location of an SNP in the pre-microRNA might alter

processing. To determine how SNPs affect microRNA processing, we performed stepwise *in vitro* maturation assays and compared the processing efficiency of wild-type and variant microRNAs by incubating wt and variant precursors with the immune-purified Drosha/DGCR8 microprocessor alone or in combination with recombinant Dicer.

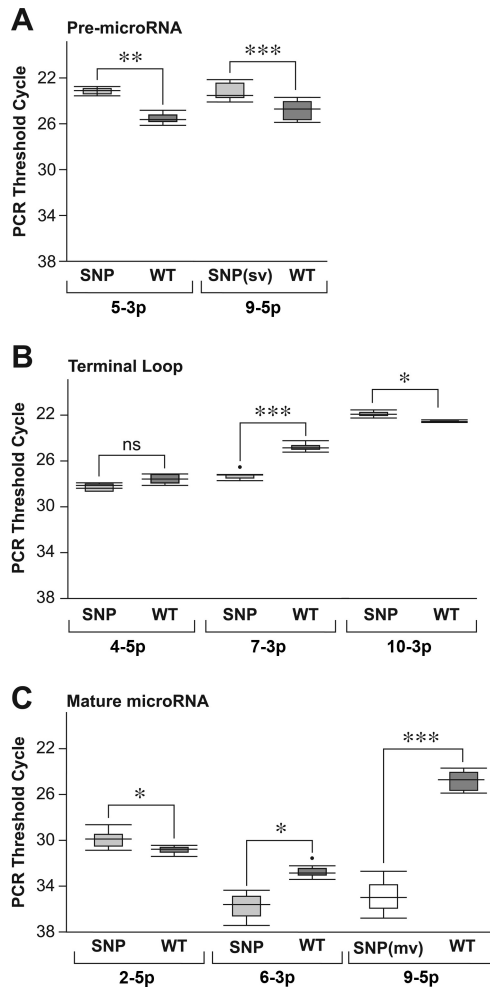We first examined SNPs in the pre-microRNA region in miR-K12-5 and -9sv. It was previously reported that miR-K12-5

A

Pre-microRNA

B

Terminal Loop

C

Mature microRNA

FIG 2 Box-and-whisker plots representing the C_T values of transduced HEK293T cells stably expressing wild-type and variant microRNA sequences. The middle 50% of the C_T values, known as the interquartile range, is inside the box. The horizontal line inside the box represents the median C_T value, and the whiskers represent 1.5 times the interquartile range on each side of the box. Any points outside the whiskers are depicted with a dot. Depiction of levels of significance are as follow: not significant (ns), $P \geq 0.01$; *, $P < 0.01$; **, $P < 0.001$; ***, $P < 0.0001$.

showed an increased microRNA maturation efficiency in BC-1 cells than in BCBL-1 cells (19), consistent with the data presented above. The mature miR-K12-5 sequence observed in BCBL-1 cells creates a bulge in the pre-microRNA stem-loop which inhibits Drosha processing (19). We tested miR-K12-5wt (BCBL-1 cells) and miR-K12-5v (BC-1 cells) (Fig. 4A, left) and confirmed that Drosha processed them with different efficiencies. We could not detect either miR-K12-5wt or miR-K12-5v in mature miR-K12-5. However, we detected Drosha processing of miR-K12-5wt at low levels (Fig. 4A); miR-K12-5wt could not be detected in a previous study (19). mir-K12-9sv contains an A-to-C change 2 nt upstream of the putative Drosha cleavage site in the 5′ arm of the pre-microRNA precursor, which should not alter folding, as predicted by M-fold software. Drosha processing and microRNA maturation were reduced by 40% in miR-K12-9sv compared to those in miR-K12-9wt (Fig. 4A). This is in contrast to the finding for HEK293T cells transduced with pre-microRNA mir-K12-9sv, in which ex-

pression of mature microRNA was increased compared to that in the wild type (Fig. 2A). The only PEL cell line that had the miR-K12-9sv sequence was VG-1, which showed a 14-fold increase in mature microRNA expression compared to that for BCBL-1 cells.

Second, we examined SNPs in miRs-K12-4, -7, and -10 that were located in the terminal loop of the pre-microRNA. The terminal loop of pre-microRNA is a critical structural feature for microprocessor/Dicer processing (27–29). In addition, the terminal loop has been shown to function as a binding site for cellular proteins, such as KSRP and hnRNP A1, which in the case of the miRNA lin-28 control microprocessor/Dicer processing in the nucleus and cytoplasm (28, 30, 31). miR-K12-4v, which has a C-to-U substitution in the terminal loop, did not have Drosha processing significantly different from that of the wt, but Dicer processing and mature microRNA yield were reduced by about 30% compared to those for the wt (Fig. 4B, left). This is consistent with the data obtained from transduced HEK293T cells. miR-K12-7v has a C-to-A SNP that disrupts a potential C-G base pairing and may result in a terminal loop more flexible than that of miR-K12-7wt (Fig. 4B, fourth panel). Several studies suggested that larger, more flexible terminal loops can affect the efficiency of both Drosha and Dicer processing (28, 29, 32). miR-K12-7v showed a slight decrease in Drosha processing (Fig. 4B) but an increase in Dicer processing compared to those for miR-K12-7wt (Fig. 4B). However, quantitative analysis of three consecutive assays could not detect a statistically significant difference in maturation between miR-K12-7v and miR-K12-7wt (Fig. 4B).

miR-K12-10v has a C-to-G SNP within the terminal loop of miR-K12-10, which was not predicted to significantly change the terminal loop structure. miR-K12-10v SNP did not differ in either microprocessor or Dicer processing compared to that for miR-K12-10wt (Fig. 4B, fifth panel).

The analysis of three SNPs within the microRNA terminal loop indicated that processing efficiency for clinically observed variant microRNA alleles cannot simply be predicted. For miR-K12-4, an SNP in the terminal loop reduced Dicer processing by 30% but had no effect on Drosha cleavage, a result consistent with results presented in a previous report demonstrating that the terminal loop is not critical for Drosha processing (27); however, similar SNPs within miR-K12-7 and -10 did not affect processing.

Third, we examined SNPs within the mature microRNA sequences. In miR-K12-2, a C-to-A SNP in miR-K12-2v created an additional A·U pair within the stem adjacent to the terminal loop (Fig. 4C, left). The efficiency of Drosha cleavage of miR-K12-2v was moderately decreased compared to that of miR-K12-2wt, and mature microRNAs were not detected for either miR-K12-2wt or miR-K12-2v (Fig. 4C, left). Interestingly, for miR-K12-2v, we detected a new RNA product of 35 nt in both the Drosha-only and Drosha/Dicer lanes (Fig. 4C, left). This product likely results from Drosha recognizing a novel cleavage site. Large terminal loops adjacent to long stems can be recognized by Drosha/DGCR8 as unstructured single-stranded (ssRNA) segments and as a result can be bound in an opposite orientation. Such alternative site usage yields small RNA products that do not give rise to mature microRNAs (24). Our data suggest that stabilization of the stem in miR-K12-2v may create an alternative Drosha processing site which would result in the 35-nt product.

The SNP in miR-K12-6 is at the 3′ end of the miR-K12-6 mature microRNA sequence. We showed very little difference in Drosha/Dicer processing efficiency between wild-type and variant
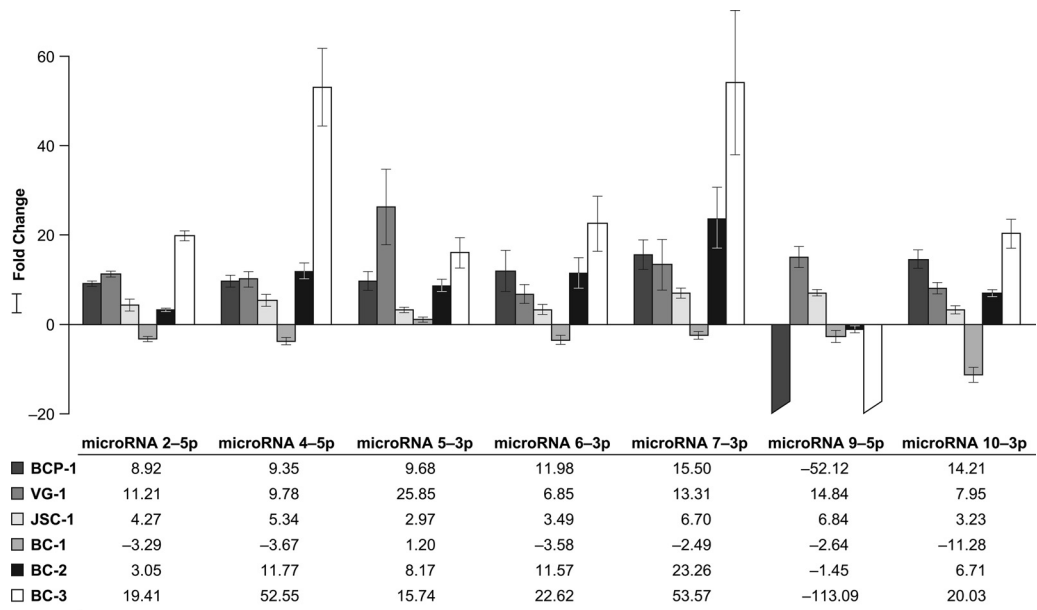
FIG 3 Applied Biosystems custom small RNA RT-PCR analysis of KSHV latently infected PEL cell lines. Mature microRNA expression levels are shown as the fold change in expression of the target genes (microRNAs) normalized to the level of expression of the internal control gene (RNU6B) and relative to the level of expression by the wild-type BCBL-1 cell line using the $2^{-\Delta\Delta CT}$ method (23). A positive fold change represents an upregulated PEL cell line, whereas a negative fold change represents a downregulated PEL cell line. The negative fold changes presented here were obtained by taking the negative inverse (i.e., -1/fold change of the result from the $2^{-\Delta\Delta CT}$ method). Standard errors were computed in the R package plotrix. These values were then used to compute interval limits (95%) on the basis of 4 degrees of freedom (3 treated sample replicates + 3 control sample replicates − 2). Values were then transformed from $\log_2$ to fold change scale by exponentiation, 2^x, where x denotes the lower limit and upper limit of the standard error values for each PEL cell line of interest compared, and appropriate standard error bars are added. The standard error bars are asymmetrical due to exponentiation.

miR-K12-6 (Fig. 4C, thrid panel), and quantification of mature microRNA showed less than a 10% decrease of mature miR-K12-6v compared to that for miR-K12-6wt (Fig. 4A). For miR-K12-9, we tested a highly variant allele, miR-K12-9mv, containing 10 SNPs located throughout the pre-microRNA, including the mature microRNA, which also severely affected folding, as predicted by M-fold. The multiple SNPs in miR-K12-9mv completely abrogated Drosha/Dicer processing, and the quantification of mature microRNA detected background levels (Fig. 4C, fifth panel). These data demonstrate not only that the multiple SNPs in the pre-microRNA precursor of miR-K12-9mv prevent miR-K12-9mv processing, consistent with the results of RT-PCR assays with both HEK293T and PEL cells, but also that the altered RNA secondary structure is not an alternative substrate for Drosha/Dicer processing.

In summary, analysis of clinically observed microRNA SNPs by performing *in vitro* maturation assays demonstrated that SNPs occurring throughout pre-microRNAs can have profound effects on microRNA maturation efficiency, ranging from the moderate decrease seen for miR-K12-6 to the total abrogation seen for miR-K12-9mv.

Analysis of luciferase microRNA reporter assays for KSHV-encoded microRNAs. We next asked whether the observed SNPs also affect microRNA silencing efficiency. To this end, we performed previously established luciferase microRNA sensor assays with recombinant expression plasmids of miR-K12-4, -6, -7, -9, and -10 under the control of the cytomegalovirus (CMV) promoter (33). To test each microRNA allele, we used microRNA sensor plasmids containing two binding sites for each wt KSHV microRNA within the 3′ untranslated region of a luciferase reporter. We excluded miR-K12-2 and -5 from this analysis because we could not detect any mature microRNAs when performing *in vitro* maturation assays (Fig. 4).

For miR-K12-4v and -9sv, reduced repression activity was observed compared to that for wt, but miRs-K12-6, -7, and -10 showed no differences. miR-K12-9mv, which was demonstrated to abrogate expression, had no silencing activity (Fig. 5). These data confirmed that altered premicroRNA sequences correspondingly affect both microRNA maturation and silencing.

DISCUSSION

Our previous sampling of KSHV microRNA sequence heterogeneity revealed that some viral microRNAs were highly conserved, while others displayed distinct sequence variability among samples from KSHV-infected patients and from a number of PEL cell lines (15). Here we functionally analyzed single- or multiple-nucleotide polymorphisms of seven KSHV microRNA genes (Table 1), some of which were predicted to have a variant secondary

TABLE 4 KSHV copy numbers in PEL lines determined by quantitative real-time PCR

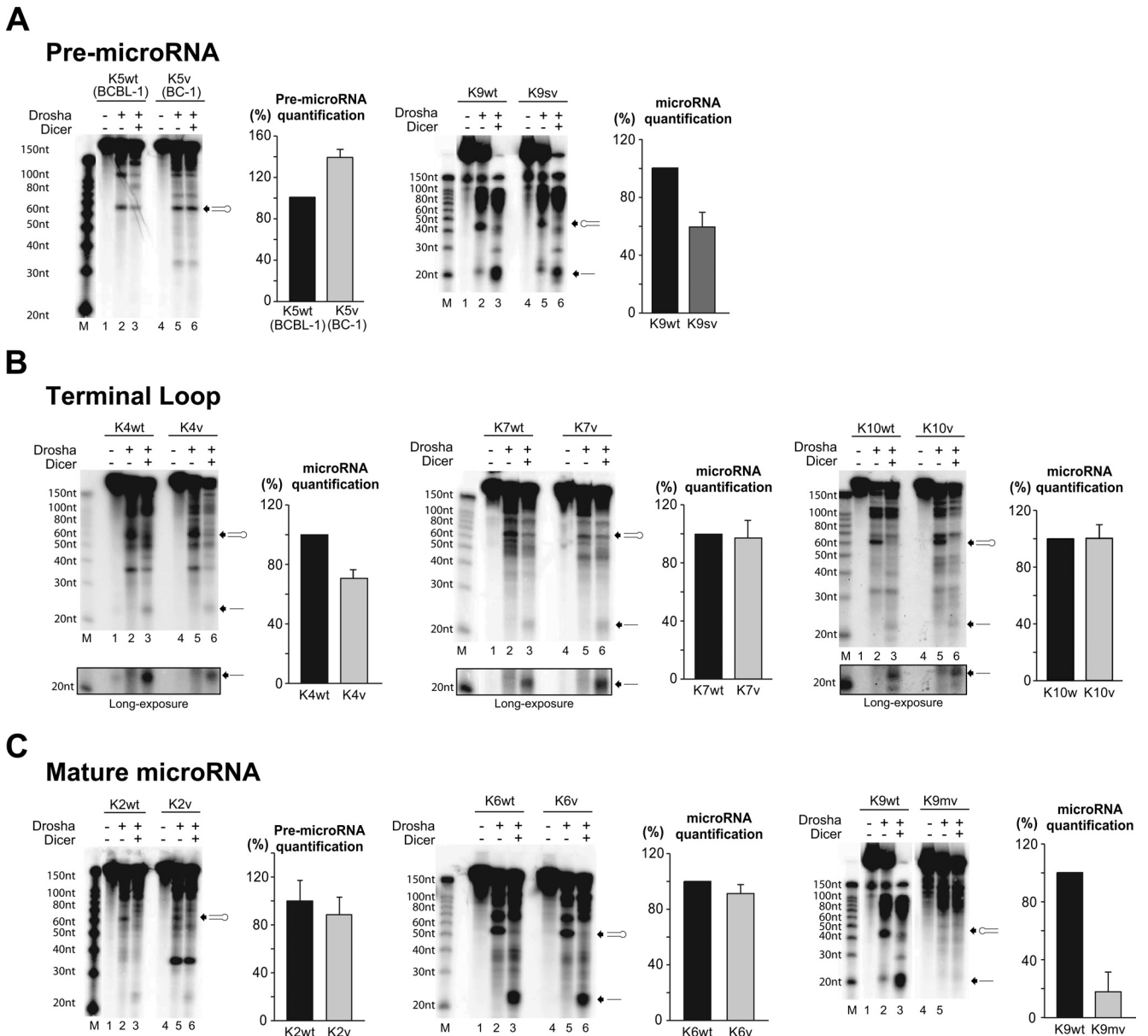| PEL cell line	KSHV copy no./reaction	No. of KSHV copies/cell
BCBL-1	8,700,000	158
BCP-1	7,800,000	164
VG-1	660,000	19
JSC-1	2,100,000	74
BC-1	4,600,000	84
BC-2	1,100,000	344
BC-3	9,000,000	486

FIG 4 A. *In vitro* maturation assay for miR-K12-5 and -9. These microRNA variants have SNPs in pre-microRNA. (First and third panels) Products on urea-polyacrylamide gel. Black arrows, pre-microRNA and microRNA produced from each processing; lanes M, molecular size markers. (Second and fourth panels) Graphs of pre-microRNA quantification normalized by the levels for the wt. Results are shown as percentages ± standard deviations from three independent experiments. (B) *In vitro* maturation assay for miR-K12-4, miR-K12-7, and miR-K12-10. The variants of these microRNAs have SNPs in different positions in the terminal loop of pre-microRNA. (First, third, and fifth panels) Products on urea-polyacrylamide gels. Black arrows, pre-microRNA and microRNA produced from each processing; lanes M, molecular size markers. (Second, fourth, and sixth panels) Graphs of pre-microRNA quantification normalized by the levels for the wt. Results are shown as percentages ± standard deviations from three independent experiments. (C) *In vitro* maturation assay for miR-K12-2, miR-K12-6, and miR-K12-9mv. The variants of these microRNAs have an SNP or SNPs within mature microRNA sequences. (First, third, and fifth panels) Products on urea-polyacrylamide gels. Black arrows, pre-microRNA produced; lanes M, molecular size markers. (Second, fourth, and sixth panels) Graphs of pre-microRNA quantification normalized by the levels for the wt. Results are shown as percentages ± standard deviations from three independent experiments.

structure of pre-microRNAs, and evaluated the genes for their expression, maturation, and targeting efficiencies. We hypothesized that clinically observed polymorphisms translate into microRNA expression differences that are associated with clinical phenotypes in KSHV-infected patients.

We generated retroviral vectors expressing either wt or variant microRNA alleles for seven microRNAs and transduced HEK293T cells. We observed both increased and decreased expression of mature viral microRNA in association with SNPs, and the magnitude of the expression difference varied in significance. The fact that all microRNAs were expressed from an identical CMV promoter within the integrated vector strongly suggested that differences in microRNA expression in this system must be due to pri- and pre-microRNA processing.
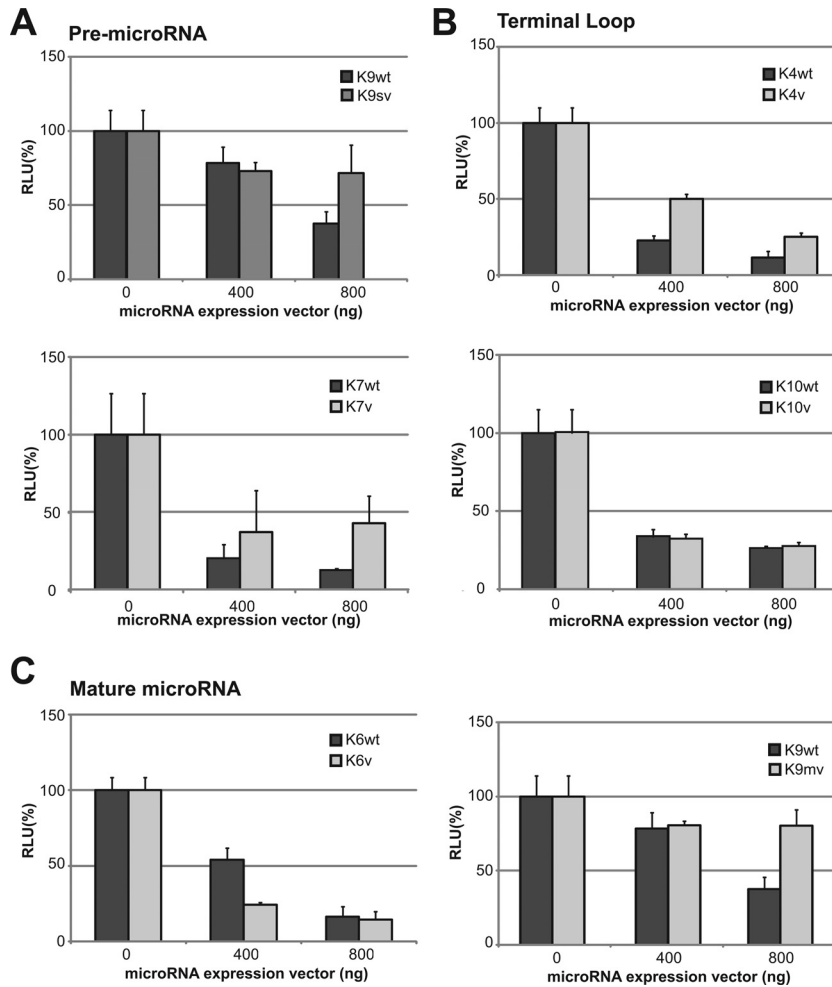
FIG 5 Luciferase-based microRNA repressor assay. The microRNA sensor vector and increasing amounts (0, 400, and 800 ng) of the microRNA expression vector were cotransfected with 10 ng of *Renilla* luciferase vector for normalization into HEK293T cells. Ratios on the *x* axes indicate the amount of microRNA expression vector, and the relative light unit (RLU) values are normalized to the value for *Renilla* luciferase and are shown as a percentage compare to the value for the wt. Empty vector was used as a negative control. Results are shown as means ± standard deviations from three independent experiments.

We also measured microRNA expression levels for the same microRNAs in seven PEL cell lines and found highly divergent expression levels. Data from these experiments suggest that in PEL cells mechanisms determining the level of expression of mature viral microRNAs are complex, and while SNPs in the pre-microRNA play a role, other factors are also important. These may include the position of the pre-microRNA within the pri-microRNA cluster, namely, SNPs outside the pre-microRNA sequence; competing effects of host or other viral microRNAs; and differential transcriptional activity between different PEL cells. Interestingly, viral copy number did not predict the microRNA expression level; for example, VG-1 cells contained the lowest number of viral copies of all PEL lines tested but expressed high viral microRNA levels.

To directly test the effect of SNPs on microRNA processing, we performed stepwise *in vitro* maturation assays and compared the processing efficiency of variant and wt microRNA alleles located at different regions of the pre-microRNAs (ssRNA-double-stranded [dsRNA] stem junction, terminal loop, and mature microRNA). Two different models for the recognition of Drosha

cleavage sites have been proposed, and both suggest that Drosha determines its cleavage site by probing RNA structural features within the pre-microRNA. In one model, Drosha detects the ssRNA-dsRNA junction and cleaves at a site ~11 nt away (27); the alternative model proposes that Drosha measures and cleaves in reference to the terminal loop (34). Both models suggest that Drosha determines its cleavage site by probing RNA structural features within the pri-microRNA. Our observation that miR-K12-9sv, which contains the SNP in the 5′ arm, shows a significant reduction in Drosha processing is consistent with sequential processing of the 5′ and 3′ cleavage sites. Thus, our data support the former junction model. Recently, Warf et al. reported that Drosha first recognizes and processes a site on the 5′ arm of the pri-microRNA and subsequently determines the cleavage site on the 3′ arm by measuring 2 nt from the cleavage site on the 5′ arm (35). Polymorphisms within the loop of miR-K12-4 reduced processing, while SNPs in miR-K12-7 and -10 had very small effects, demonstrating that the effect of sequence variations on loop processing cannot simply be predicted. This was equally true for miR-K12-5, for which a polymorphism led to more efficient processing, and

for miR-K12-2, where a polymorphism may create an alternate Drosha cleavage site, thereby preventing the formation of the mature microRNA. The latter was also the case for miR-K12-9mv, where multiple SNPs completely abrogated processing (Fig. 4).

The phenotypic consequences of these observed microRNA maturation differences can fall into three major conceptual classes. First, as observed for miR-K12-9mv, complete abrogation of expression could lead to target genes that are targeted in wt infected cells not being downregulated. Second, the effect of decreased processing is less clear since it depends on whether the particular microRNA is expressed at high or low levels. For example, miR-K12-5, which is expressed at very low levels in BCBL-1, may regulate more genes in BC-1 cells, where it is robustly expressed, or may silence target genes more efficiently. In clinical samples, the majority of sequences encode the miR-K12-5v SNP, resulting in poor expression, perhaps suggesting evolutionary selection. A third aspect concerns SNPs that affect the functional domain or seed sequence (nt 2 to 8) of the mature microRNA, since such SNPs may or may not affect maturation but may potentially change the targeting specificity.

An important question is whether the observed KSHV microRNA SNPs and their associated expression differences have phenotypic consequences with respect to disease type, onset, and/or progression in KSHV-infected subjects. To address this question, it is important to understand (i) which microRNA-targeted genes are important for pathogenesis and (ii) which SNP-driven expression differences affect these targets. With respect to targeting, a number of reports have identified and confirmed specific cellular and viral genes targeted by KSHV microRNAs, including those under study here (for a review, see the work of Haecker et al. [26]). More recently, KSHV microRNA targetomes have been analyzed in several PEL cell lines using high-throughput sequencing of RNA–UV cross-linking and immunoprecipitation and photoactivatable-ribonucleoside-enhanced UV cross-linking and immunoprecipitation methods (26, 36). In BCBL-1 and BC-3 cells, 1,170 and 950 genes, respectively, have been identified as putative targets (26). Collectively, these studies have pointed to key regulatory pathways, such as inhibition of apoptosis, cell cycle control, immune evasion, and cytokine signaling, all central to KSHV biology and pathogenesis. For example, IRAK-1 has been identified as a target of miR-K12-9. The complete loss of this microRNA in BC-3 cells or in infected subjects due to multiple SNPs may affect the Toll-like receptor/IL1R. Similarly, miR-K4 has been shown to downregulate caspase 3, making cells less resistant to apoptotic stimuli (37). Polymorphisms in miR-K12-5, which strongly affected processing, could affect MYD88, IL2RB, and CDK16 signaling.

Reports of three studies using different experimental systems indicated that miR-K12-9 can reduce the expression of the replication-transcription activator (RTA) of KSHV by direct targeting (38–40). Moreover, miR-K12-5 has also been implicated in regulating RTA. It is interesting to note that BCBL-1, which expresses very low to undetectable levels of miR-K12-5, has a high spontaneous KSHV reactivation rate. Thus, differential microRNA maturation of miR-K12-9 and miR-K12-5 may contribute to latency control. Interestingly, two KSHV-associated diseases, MCD and the recently identified KICS, are characterized by lytic replication rather than the tight latency observed in KS and PEL (18). We recently reported that SNPs within miR-K12-4, -5, -6, and -7 are statistically significantly associated with MCD/KICS risk. Of note,

while the reported overall frequency of SNPs within human microRNA is low (41), several reports have identified specific microRNA SNPs in colorectal cancer that have been evaluated as potential biomarkers (42). Although human microRNA SNPs were not the focus of this study, it is worth investigating any compounding effects of potential human microRNA SNPs in the context of KSHV infection.

In summary, we have demonstrated that a number of SNPs within all three KSHV pre-microRNA domains observed in clinical subjects can have profound but not always predictable effects on microRNA maturation. These observations are of interest for cancer biology beyond KS, since many human tumors display altered microRNA expression profiles (for a review, see reference 43). To date, relatively little is known about the frequencies of polymorphisms in human microRNAs in cancer, and it is important to note that some microRNAs classified as deregulated may contain SNPs, thereby escaping detection through the most commonly used TaqMan PCR arrays. Moreover, deep sequencing of small RNA libraries has identified many offset 5′ processing events, which further expand targeting specificity.

REFERENCES

1. **Chang Y, Cesarman E, Pessin MS, Lee F, Culpepper J, Knowles DM, Moore PS.** 1994. Identification of herpesvirus-like DNA sequences in AIDS-associated Kaposi's sarcoma. Science **266:**1865–1869.
2. **Cesarman E, Chang Y, Moore PS, Said JW, Knowles DM.** 1995. Kaposi's sarcoma-associated herpesvirus-like DNA sequences in AIDS-related body-cavity-based lymphomas. N. Engl. J. Med. **332:**1186–1191.
3. **Soulier J, Grollet L, Oksenhendler E, Cacoub P, Cazals-Hatem D, Babinet P, d'Agay MF, Clauvel JP, Raphael M, Degos L, Sigaux F.** 1995. Kaposi's sarcoma-associated herpesvirus-like DNA sequences in multicentric Castleman's disease. Blood **86:**1276–1280.
4. **Ambros V.** 2004. The functions of animal microRNAs. Nature **431:**350–355.
5. **Bartel DP.** 2004. MicroRNAs: genomics, biogenesis, mechanism, and function. Cell **116:**281–297.
6. **Pfeffer S, Sewer A, Lagos-Quintana M, Sheridan R, Sander C, Grasser FA, van Dyk LF, Ho CK, Shuman S, Chien M, Russo JJ, Ju J, Randall G, Lindenbach BD, Rice CM, Simon V, Ho DD, Zavolan M, Tuschl T.** 2005. Identification of microRNAs of the herpesvirus family. Nat. Methods **2:**269–276.
7. **Boss IW, Plaisance KB, Renne R.** 2009. Role of virus-encoded microRNAs in herpesvirus biology. Trends Microbiol. **17:**544–553.
8. **Cai X, Lu S, Zhang Z, Gonzalez CM, Damania B, Cullen BR.** 2005. Kaposi's sarcoma-associated herpesvirus expresses an array of viral microRNAs in latently infected cells. Proc. Natl. Acad. Sci. U. S. A. **102:**5570–5575.
9. **Grundhoff A, Sullivan CS, Ganem D.** 2006. A combined computational and microarray-based approach identifies novel microRNAs encoded by human gamma-herpesviruses. RNA **12:**733–750.
10. **Lin YT, Kincaid RP, Arasappan D, Dowd SE, Hunicke-Smith SP, Sullivan CS.** 2010. Small RNA profiling reveals antisense transcription throughout the KSHV genome and novel small RNAs. RNA **16:**1540–1558.
11. **Samols MA, Hu J, Skalsky RL, Renne R.** 2005. Cloning and identification of a microRNA cluster within the latency-associated region of Kaposi's sarcoma-associated herpesvirus. J. Virol. **79:**9301–9305.
12. **Umbach JL, Cullen BR.** 2010. In-depth analysis of Kaposi's sarcoma-

associated herpesvirus microRNA expression provides insights into the mammalian microRNA-processing machinery. J. Virol. **84:**695–703.

13. **O'Hara AJ, Chugh P, Wang L, Netto EM, Luz E, Harrington WJ, Dezube BJ, Damania B, Dittmer DP.** 2009. Pre-micro RNA signatures delineate stages of endothelial cell transformation in Kaposi sarcoma. PLoS Pathog. **5:**e1000389. doi:10.1371/journal.ppat.1000389.

14. **O'Hara AJ, Vahrson W, Dittmer DP.** 2008. Gene alteration and precursor and mature microRNA transcription changes contribute to the miRNA signature of primary effusion lymphoma. Blood **111:**2347–2353.

15. **Marshall V, Parks T, Bagni R, Wang CD, Samols MA, Hu J, Wyvil KM, Aleman K, Little RF, Yarchoan R, Renne R, Whitby D.** 2007. Conservation of virally encoded microRNAs in Kaposi sarcoma-associated herpesvirus in primary effusion lymphoma cell lines and in patients with Kaposi sarcoma or multicentric Castleman disease. J. Infect. Dis. **195:**645–659.

16. **Marshall V, Martro E, Labo N, Ray A, Wang D, Mbisa G, Bagni RK, Volfovsky N, Casabona J, Whitby D.** 2010. Kaposi sarcoma (KS)-associated herpesvirus microRNA sequence analysis and KS risk in a European AIDS-KS case control study. J. Infect. Dis. **202:**1126–1135.

17. **Ray A, Marshall V, Uldrick T, Leighty R, Labo N, Wyvill K, Aleman K, Polizzotto MN, Little RF, Yarchoan R, Whitby D.** 2012. Sequence analysis of Kaposi sarcoma-associated herpesvirus (KSHV) microRNAs in patients with multicentric Castleman disease and KSHV-associated inflammatory cytokine syndrome. J. Infect. Dis. **205:**1665–1676.

18. **Uldrick TS, Wang V, O'Mahony D, Aleman K, Wyvill KM, Marshall V, Steinberg SM, Pittaluga S, Maric I, Whitby D, Tosato G, Little RF, Yarchoan R.** 2010. An interleukin-6-related systemic inflammatory syndrome in patients co-infected with Kaposi sarcoma-associated herpesvirus and HIV but without multicentric Castleman disease. Clin. Infect. Dis. **51:**350–358.

19. **Gottwein E, Cai X, Cullen BR.** 2006. A novel assay for viral microRNA function identifies a single nucleotide polymorphism that affects Drosha processing. J. Virol. **80:**5321–5326.

20. **de Sanjose S, Marshall V, Sola J, Palacio V, Almirall R, Goedert JJ, Bosch FX, Whitby D.** 2002. Prevalence of Kaposi's sarcoma-associated herpesvirus infection in sex workers and women from the general population in Spain. Int. J. Cancer **98:**155–158.

21. **Yuan CC, Miley W, Waters D.** 2001. A quantification of human cells using an ERV-3 real time PCR assay. J. Virol. Methods **91:**109–117.

22. **Kutner RH, Zhang XY, Reiser J.** 2009. Production, concentration and titration of pseudotyped HIV-1-based lentiviral vectors. Nat. Protoc. **4:**495–505.

23. **Livak KJ, Schmittgen TD.** 2001. Analysis of relative gene expression data using real-time quantitative PCR and the 2($-$delta delta C(T)) method. Methods **25:**402–408.

24. **Lee Y, Kim VN.** 2007. In vitro and in vivo assays for the activity of Drosha complex. Methods Enzymol. **427:**89–106.

25. **Samols MA, Skalsky RL, Maldonado AM, Riva A, Lopez MC, Baker HV, Renne R.** 2007. Identification of cellular genes targeted by KSHV-encoded microRNAs. PLoS Pathog. **3:**e65. doi:10.1371/journal.ppat.0030065.

26. **Haecker I, Gay LA, Yang Y, Hu J, Morse AM, McIntyre LM, Renne R.** 2012. Ago HITS-CLIP expands understanding of Kaposi's sarcoma-associated herpesvirus miRNA function in primary effusion lymphomas. PLoS Pathog. **8:**e1002884. doi:10.1371/journal.ppat.1002884.

27. **Han J, Lee Y, Yeom KH, Nam JW, Heo I, Rhee JK, Sohn SY, Cho Y,** Zhang BT, Kim VN. 2006. Molecular basis for the recognition of primary microRNAs by the Drosha-DGCR8 complex. Cell **125:**887–901.

28. **Michlewski G, Guil S, Semple CA, Caceres JF.** 2008. Posttranscriptional regulation of miRNAs harboring conserved terminal loops. Mol. Cell **32:**383–393.

29. **Zhang X, Zeng Y.** 2010. The terminal loop region controls microRNA processing by Drosha and Dicer. Nucleic Acids Res. **38:**7689–7697.

30. **Michlewski G, Caceres JF.** 2010. Antagonistic role of hnRNP A1 and KSRP in the regulation of let-7a biogenesis. Nat. Struct. Mol. Biol. **17:** 1011–1018.

31. **Trabucchi M, Briata P, Garcia-Mayoral M, Haase AD, Filipowicz W, Ramos A, Gherzi R, Rosenfeld MG.** 2009. The RNA-binding protein KSRP promotes the biogenesis of a subset of microRNAs. Nature **459:** 1010–1014.

32. **Zeng Y, Cullen BR.** 2005. Efficient processing of primary microRNA hairpins by Drosha requires flanking nonstructured RNA sequences. J. Biol. Chem. **280:**27595–27603.

33. **Skalsky RL, Samols MA, Plaisance KB, Boss IW, Riva A, Lopez MC, Baker HV, Renne R.** 2007. Kaposi's sarcoma-associated herpesvirus encodes an ortholog of miR-155. J. Virol. **81:**12836–12845.

34. **Zeng Y, Yi R, Cullen BR.** 2005. Recognition and cleavage of primary microRNA precursors by the nuclear processing enzyme Drosha. EMBO J. **24:**138–148.

35. **Warf MB, Johnson WE, Bass BL.** 2011. Improved annotation of C. elegans microRNAs by deep sequencing reveals structures associated with processing by Drosha and Dicer. RNA **17:**563–577.

36. **Gottwein E, Corcoran DL, Mukherjee N, Skalsky RL, Hafner M, Nusbaum JD, Shamulailatpam P, Love CL, Dave SS, Tuschl T, Ohler U, Cullen BR.** 2011. Viral microRNA targetome of KSHV-infected primary effusion lymphoma cell lines. Cell Host Microbe **10:**515–526.

37. **Suffert G, Malterer G, Hausser J, Viiliainen J, Fender A, Contrant M, Ivacevic T, Benes V, Gros F, Voinnet O, Zavolan M, Ojala PM, Haas JG, Pfeffer S.** 2011. Kaposi's sarcoma herpesvirus microRNAs target caspase 3 and regulate apoptosis. PLoS Pathog. **7:**e1002405. doi:10.1371/journal.ppat.1002405.

38. **Bellare P, Ganem D.** 2009. Regulation of KSHV lytic switch protein expression by a virus-encoded microRNA: an evolutionary adaptation that fine-tunes lytic reactivation. Cell Host Microbe **6:**570–575.

39. **Lin X, Liang D, He Z, Deng Q, Robertson ES, Lan K.** 2011. miR-K12-7-5p encoded by Kaposi's sarcoma-associated herpesvirus stabilizes the latent state by targeting viral ORF50/RTA. PLoS One **6:**e16224. doi:10.1371/journal.pone.0016224.

40. **Ziegelbauer J, Grundhoff A, Ganem D.** 2006. Exploring the DNA binding interactions of the Kaposi's sarcoma-associated herpesvirus lytic switch protein by selective amplification of bound sequences in vitro. J. Virol. **80:**2958–2967.

41. **Saunders MA, Liang H, Li WH.** 2007. Human polymorphism at microRNAs and microRNA target sites. Proc. Natl. Acad. Sci. U. S. A. **104:**3300–3305.

42. **Zarate R, Boni V, Bandres E, Garcia-Foncillas J.** 2012. MiRNAs and LincRNAs: could they be considered as biomarkers in colorectal cancer? Int. J. Mol. Sci. **13:**840–865.

43. **Calin GA, Croce CM.** 2006. MicroRNA signatures in human cancers. Nat. Rev. Cancer **6:**857–866.